Field Observations of the Bering Sea Ice Edge Properties during March 1979

JANE BAUER AND SEELYE MARTIN

Department of Oceanography, University of Washington, Seattle 98195

(Manuscript received 5 February 1980, in final form 15 July 1980)

ABSTRACT

During March 1979 field observations in the Bering Sea show that because of the interaction of winds and ocean swell with the ice, the ice edge divides into three distinct zones. First, adjacent to the open ocean is an "edge" zone, 1–15 km in width, which consists of heavily rafted and ridged floes with thicknesses of 1–5 m and measuring 10–20 m on a side. Second is a "transition" zone measuring ~5 km in width, which consists of rectangular ice floes with thicknesses of ~0.5 m and measuring 20–40 m on a side. Third is the "interior" zone, which extends over hundreds of kilometers and consists of very large, relatively flat floes with thicknesses of ~0.3 m. In the edge zone the incident swell causes the floes to fracture, raft and form pressure ridges, resulting in small thick floes. In the transition zone the swell amplitude is reduced to the point that the floes fracture in a rectangular pattern with very little rafting or ridging taking place. In the interior zone the swell amplitude is further reduced such that the waves propagate without fracturing the ice, so that the floes have horizontal dimensions of kilometers. Because of this ice distribution, when strong winds blow off the ice, bands of ice floes form at the ice edge. The reason bands form is that the edge zone ice has a large aerodynamic drag due to the heavy rafting and ridging, so that this ice moves downwind ahead of the rest of the pack. Once this ice moves away from the pack, the combination of aerodynamic drag plus the absorption of wind wave and swell energy leads to the band formation. We observed that these bands, which are on the order of 1 km wide and 10 km in length, move south into warmer water until they melt.

1. Introduction

Observations made during a field study in March 1979 at the Bering Sea ice edge show that the interaction of ocean waves and wind contributes to ice edge properties. The discussion of these observations divides into two parts. In the first, we show that the ice adjacent to open water divides into three zones, which we call the edge, transition and interior zones, following Squire and Moore (1980). In the second, we show that during periods of off-ice winds, the combination of the increased aerodynamic roughness of the edge zone and the absorption and reflection of wind-waves and swell leads to the formation of long, linear bands of ice, measuring about 10 km in length and 1 km in width. These bands form at angles nearly perpendicular to the wind and move southwest ahead of the pack ice. Observations of the formation and movement of a single band show that the band moved southwest ~30 km into warmer water while the pack advanced only ~10 km.

2. The nature of the ice edge

During an Outer Continental Shelf Environmental Assessment Program (OCSEAP) cruise in March 1979, Martin and Kauffman (1979) took ice cores using a helicopter operating from the NOAA ship *Surveyor*. Fig. 1 shows the locations of these cores, where the southern most stations show the location of the ice edge. In this section we discuss the ice edge properties based on the traverse lines labeled W, B and C, which were occupied on 6, 7 and 9 March, respectively. First, we discuss the general properties of the ice edge, then document the specific ice properties observed on the three traverse lines.

To review the general ice properties, Fig. 2 shows a schematic diagram in both plan and side view of the three kinds of ice. First, at the outer edge of the pack, there is open water. Then, the edge zone which is 5–15 km wide, consists of small broken floes which are ~10–20 m in diameter. In cross-section, these floes are heavily rafted and ridged, with sail heights of up to 1 m and keel depths of 2–4 m. Figs. 3a and 3b show from photographs taken on 9 March, an aerial and surface view of the ice near the edge. The ridge in the foreground of Fig. 3b, which is 1 m high and made up of ice 0.1–0.2 m thick, is shown from the air in the center foreground of Fig. 3a. The reason for the heavy rafting and ridging in the edge zone is that both ocean swell and wind act on the floes to work them against one another. Squire and Moore (1980) show from data taken on the same cruise that the swell propagates at least 65 km into

0027-0644/80/122045-12$07.00

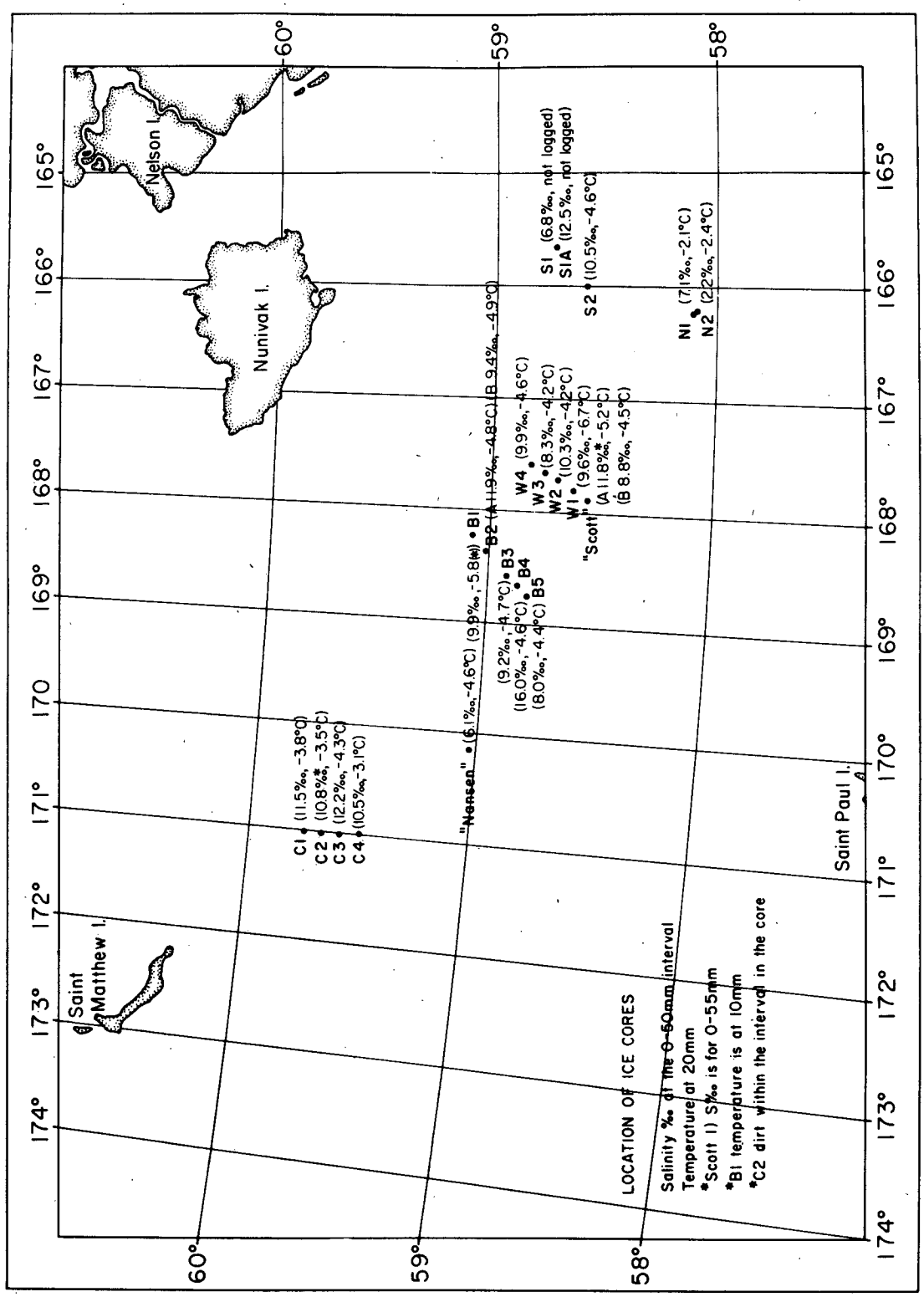

FIG. 1. Chart showing the location of all ice cores taken during the March 1979 *Surveyor* cruise (chart courtesy Carol Pease).

the pack. From their data, the observed predominant wave period was 8–10 s, which yields a wavelength of 100–160 m, so that the 20 m floe diameter is a fraction of a wavelength.

Second, the transition zone, which is ~5 km wide, is characterized by a rectangular pattern. Figs. 7a and 11 show the most dramatic examples of this patterned ice, which consists of rectangles measuring ~20 m in width and 40 m in length, with their long axis perpendicular to the direction of wave propagation. In cross section, this ice is about 0.3–0.6 m thick, where the thicker floes consist of two or three rafted pieces. This zone exists because the outer ice zone reduces the swell amplitude to the point that here, the waves fracture the ice without heavily rafting or ridging it.

At the inside edge of the transition zone, we observe an abrupt transition from the patterned ice to large floes measuring kilometers in extent. This third, interior zone, is the region of large floes where the swell amplitude is reduced to the point that it propagates elastically without fracturing the ice. Fig. 8a shows an aerial view of this ice, where the floes measure kilometers in extent, and 0.2–0.3 m in thickness. Satellite images suggest that this zone extends far to the north. In support of this general ice edge picture, we next examine the specific properties along the three traverse lines.

a. Line W

The W traverse took place on 6 March at the positions shown on Fig. 1. The wind on this day was negligible and the air temperature was about

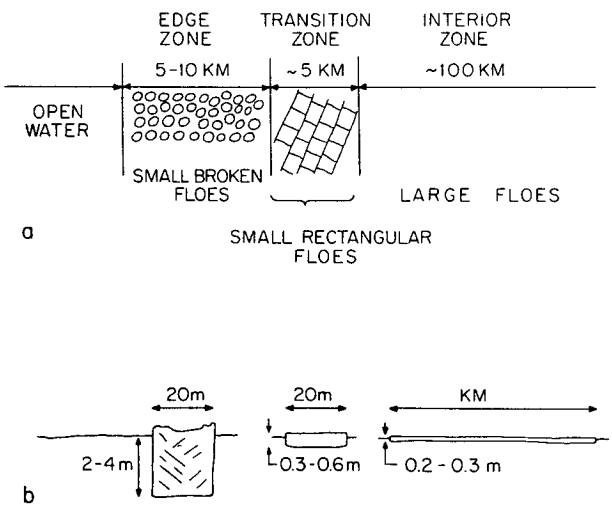

FIG. 2. A schematic diagram of the three kinds of ice which occur near the ice edge, proceeding inward from open water. The upper part of the figure shows the ice in plan view; the lower part, in side view.

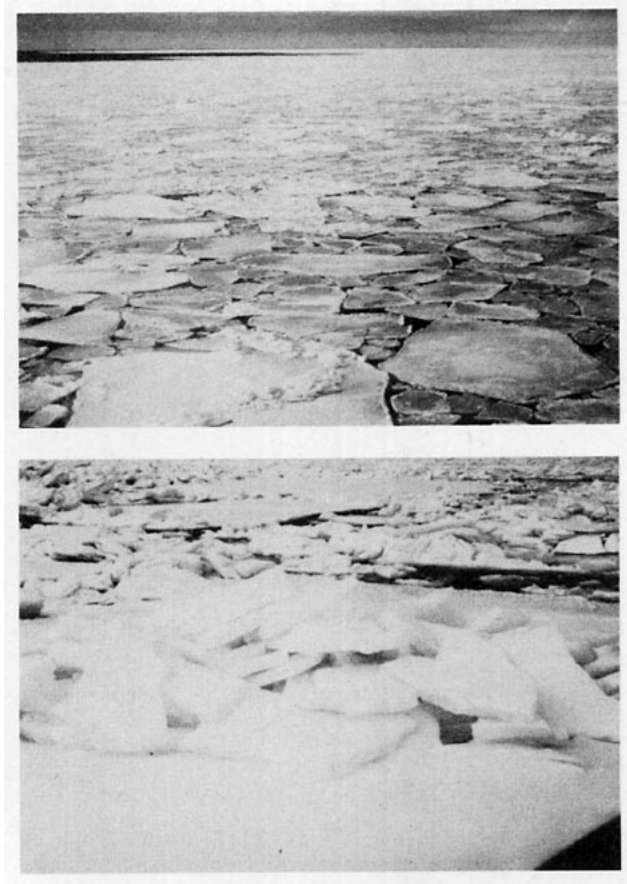

FIG. 3. Floes in the edge zone. (a) aerial view; (b) surface photograph of the ridge in the foreground of (a). See text for further explanation.

−5°C. Fig. 4 shows a schematic diagram of the kinds of ice observed on the traverse; the ice consisted of an 8 km wide edge zone and a 3 km wide transition zone with an abrupt transition from the rectangular floes to the interior zone at the northern edge of the transition zone.

The outermost floe on this line was station Scott. We had divers from the ship survey the bottom ice profile. Fig. 5a shows an oblique aerial photograph from a 60 m altitude of Scott preceding the diving. The dark area toward the camera is called the beach, and a small ridge-crack system runs horizontally in the photograph across the floe. The floe measured about 23 m by 37 m. Fig. 5b shows a surface photograph of the floe sighting down the ridge-crack system toward the beach; other ridged floes are visible in the background. We deliberately chose this floe because it was flat, as opposed to some of the heavily ridged surrounding floes. In contrast, the under-ice topography proved to be very rough. To illustrate, Fig. 6a is a map of the surface showing the survey lines DEC and BEA, with the dashed line

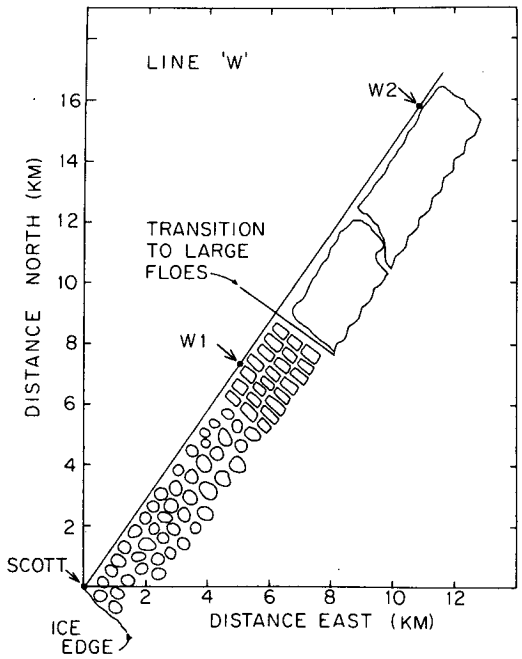

FIG. 4. A schematic diagram of the kinds of ice observed along line W. The circles indicate edge zone ice; the small squares, transition zone ice. Stations Scott, W1 and W2 show coring site locations.

showing the approximate position where the floe fractured preceding the diving. Fig. 6b shows the ice thickness from the two under-ice traverses. These observations showed that the bottom was very rough with a maximum depth of 3.5 m.

Second, Fig. 7a shows an aerial photograph of the floes at station W1 in the transition zone. These floes measured 10–25 m on a side; the one on which we landed had a thickness of 0.66 m and showed evidence of rafting at depths of 0.23 and 0.51 m. Fig. 7b shows a surface view from our floe; the pressure ridges behind the helicopter had a height of ~1 m. When we landed on the floe, we could feel the ocean swell propagating through the ice and see the swell-induced relative motion of the surrounding floes. Third, in the interior zone, Fig. 8a shows an aerial photograph of site W2 from an altitude of 150 m, where we landed on the large floe shown in the center of the photograph. The ice further in from this station also resembled this floe; namely the floes were large and flat, with low-amplitude swell propagating through them. Fig. 8b shows the surface view; the ice was 0.24 m thick and covered by ~5 mm of snow.

b. Line B

The B traverse took place on the following day, 7 March, at the positions shown on Fig. 1. As on the previous day, the wind was negligible and the air temperature was about −5°C. Fig. 9 is a sketch of the ice properties along the traverse line; again, the ice consisted of an edge zone measuring about 13 km wide and a 3 km wide transition zone with an abrupt transition from the rectangular floes to the large, interior floes.

The first station occupied was a floe next to the ship in the edge zone. Again, the floes measured 10–20 m in width, and coring observations showed that its thickness was greater than 1 m. Many of the floes seen near the ship had wetted surfaces, which are caused by the swell washing water onto the ice surface. For station B5 in the edge zone, the floe on which we landed measured ~20 m across and had a thickness of 0.34 m. Most of the surrounding floes were again rough and ridged. Moving farther into the pack, the rectangular broken ice pattern became very prominent. Finally, at station B4 in the interior zone, the ice again consisted of large flat floes which measured 0.26 m thick. Most of the floes observed

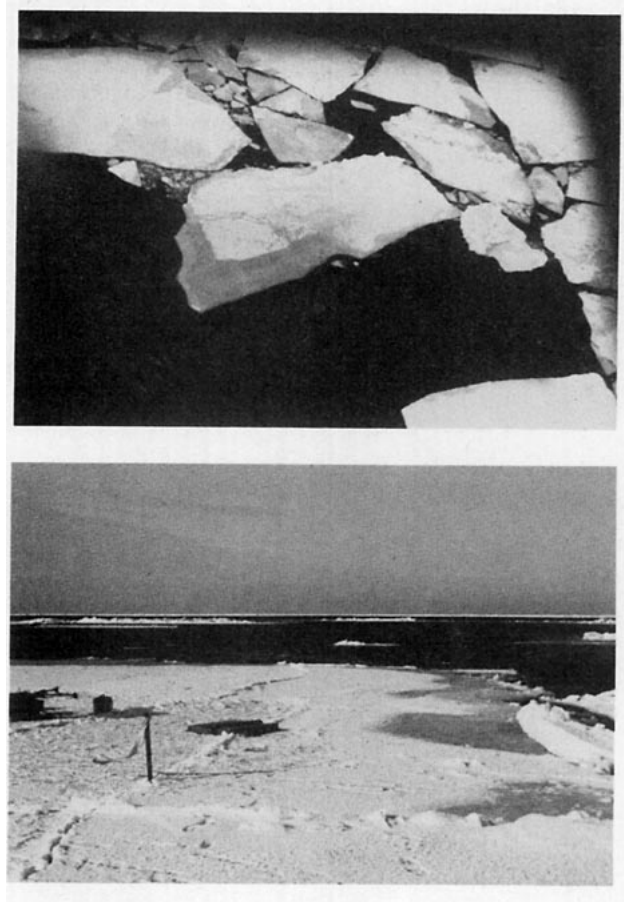

FIG. 5. Floe Scott. (a) An oblique aerial photograph from 60 m. Dark area toward camera is called the beach; small ridgecrack line runs horizontally across the floe. (b) Surface view sighting down the ridge-crack line toward the beach.

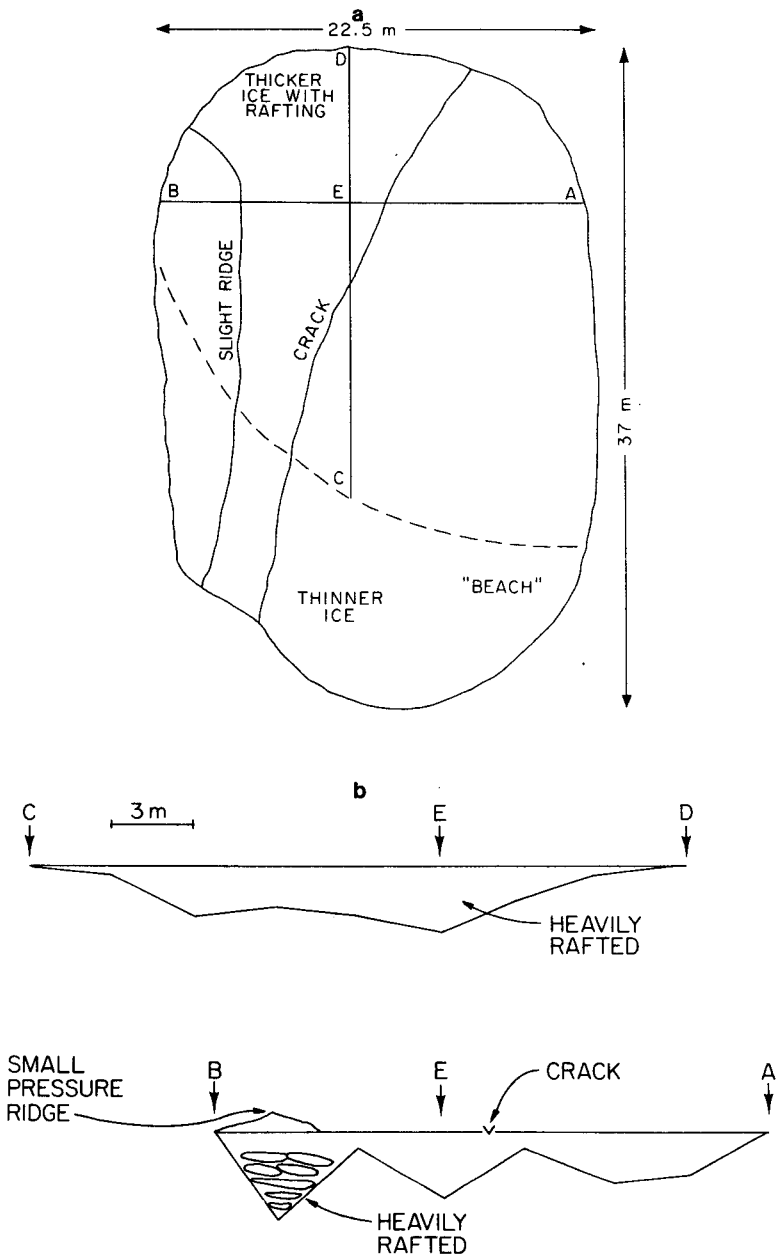

FIG. 6. The shape of floe Scott: (a) surface map of Scott (courtesy Vernon Squire); (b) two under-ice cross sections of Scott. Letters A, B, C, D and E on cross sections refer to survey lines on (6a).

on this traverse also had wetted edges. This traverse line again shows that the thickest floes occur at the ice edge.

c. Line C

The C traverse took place on 9 March 1979. On 8 March the weather deteriorated, consisting of blowing snow from the northeast with air temperatures of -1 to -3°C. On 9 March, the wind was 5.5 m s^{-1} from the northeast at temperatures between -4 and -5°C. The ice was beginning to rot, and there was a strong southerly swell propagating into the pack. Fig. 10 shows the traverse line. Because of the wind, the ice was more open along the line, and the smooth progression from small floes to large floes as we flew north was not evident. Rather, the ice consisted of bands of open

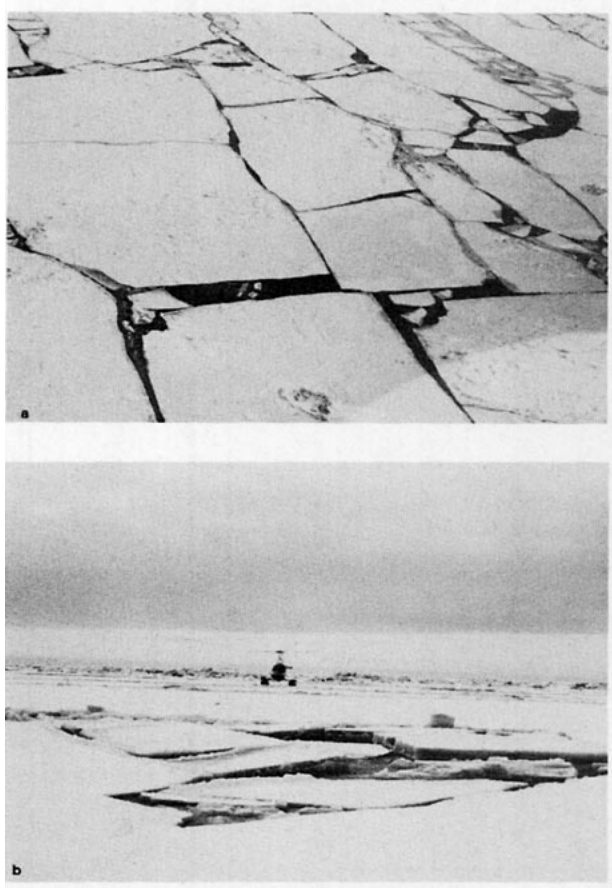

FIG. 7. Site W1. (a) Aerial photograph from 75 m of nearby floes; (b) surface photograph.

water and intermingled large and small floes for the first 30 km, at which point we reached the interior zone. We landed at two stations on the traverse line, C4 and C3.

C4 was a large floe consisting of ice which was mushy except in the bottom few centimeters, measuring 0.16 m thick with a minimum ice temperature of −3.1°C. On the floe surface, large amplitude 8 s waves propagated through the ice on which we stood. For contrast, station C3 was on a large floe immediately adjacent to the rectangular broken ice; Fig. 11 shows an aerial view from an altitude of 150 m. This picture shows rectangular floes being broken off by the swell from the large floe, where the long axis of the rectangular floes is at right angles to the direction of swell propagation. We landed on the large floe in the left foreground of Fig. 11 to observe that the ice was not mushy and measured 0.33 m thick, with a minimum ice temperature of −4.3°C. Therefore, the apparent cause of the floe distribution in Fig. 11 is that when the thin floes are warm, they are more elastic, so that the swell propagates through them without fracturing them, whereas the colder thicker floes, as shown in Fig. 11, fracture as the swell passes through them.

3. The formation and movement of the ice edge bands

a. Introduction

One effect of the ice distribution described in the previous section is that it leads to the formation of ice edge bands. Muench and Charnell (1977) review the satellite observations of the bands of ice which form at the edge of the Bering Sea pack ice during periods of off-ice winds. They show from analysis of satellite data that these bands have lengths on the order of 10 km, widths on the order of 1 km, and that the long axes of these bands are generally oriented at 40–90° to the left of the wind. They speculate that these bands form due to surface convergences caused by atmospheric roll vortices.

These bands also form at the edge of ice packs in other seas; Campbell *et al.* (1977, Fig. 5) document their formation in January 1974 in the Gulf of St. Lawrence from Skylab photographs; and S. Martin has seen NOAA imagery of their formation at the edge of the Antarctic pack ice. As an example of these bands, Fig. 12 is an aerial photograph taken from the NASA Convair-990 over the Bering Sea in 1973, Julian day 60, 00 h, 06 min, 30 s at 59.87°N, 175.063°W (from Anonymous, 1973). The aircraft

FIG. 8. Site W2. (a) Aerial photograph from 150 m; (b) surface photograph.

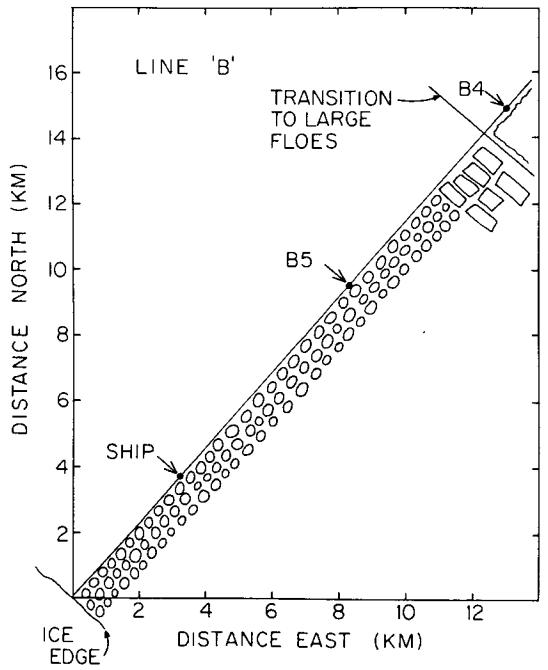

FIG. 9. A schematic diagram of the kinds of ice observed along line B. Arrows mark the coring stations; see also legend for Fig. 4.

heading was 002–004°, and its altitude was 10.5 km with 70° field-of-view, so that the picture measures 14.7 km across.

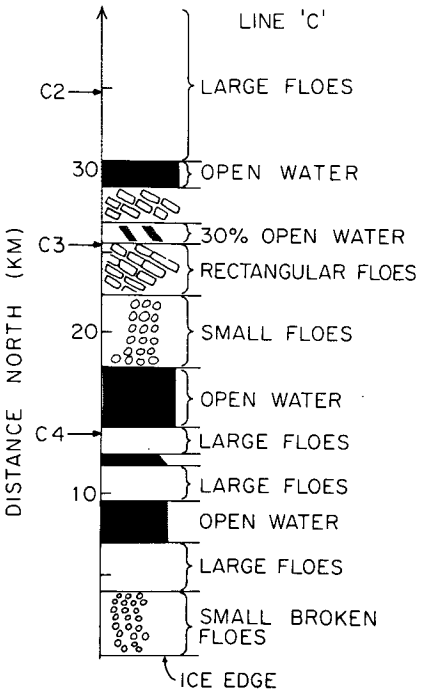

FIG. 10. A schematic diagram of the kinds of ice observed along Line C. The scale is half that of Figs. 4 and 9. The region marked 30% open water above Station C3 consisted of large floes with leads.

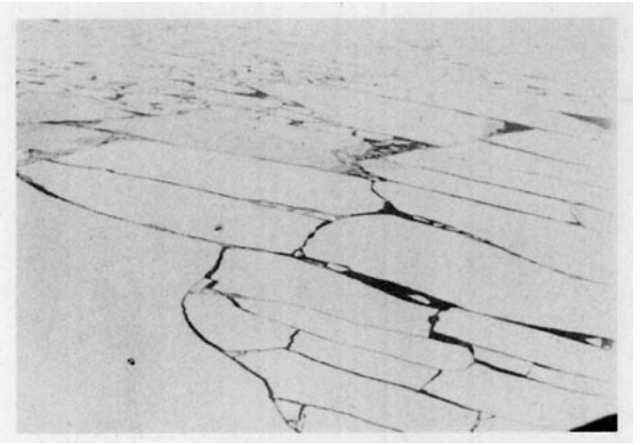

FIG. 11. Site C3. Aerial view from 150 m of floes broken by swell adjacent to large floes on which we landed. Helicopter antenna is at lower right.

The picture shows that beneath the cloud bands which are aligned approximately parallel to the wind, ice bands are visible with their long axes aligned at approximately right angles to the wind. At their widest point, the bands are ~0.6 km wide, and are 10–13 km long. For the same day, Gloersen and LaViolette (1974) show the surface pressure map and a U.S. Air Force Weather Service Satellite image of the Bering Sea ice. The satellite image shows numerous ice bands at the edge; the weather map shows that the winds are approximately from the northeast. Coast Guard weather data gathered at the same time (from Campbell *et al.*, 1975) shows that the surface air temperature was −10°C and the wind speed was 5 m s^{-1}.

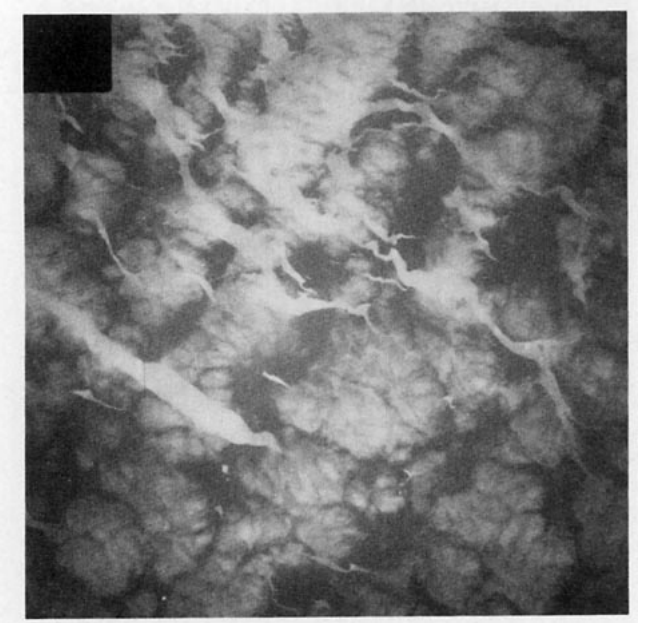

FIG. 12. Aerial photograph from 10.5 km of the ice edge bands; north is to the top. See text for further explanation, photograph courtesy NASA.

FIG. 13. Aerial view of the green floe; panel measures 1 m × 2 m.

How do these bands form? In the previous section, we showed that the effect of the wind and waves at the ice edge was to work the ice in the edge zone so that it consists of numerous small floes, which are heavily rafted and ridged. Therefore, the pack ice has an outer zone of much thicker ice, with considerable top and bottom topography, adjacent to the open water. We carried out from the *Surveyor* a field experiment during a period of off-ice winds to study the movement of this thicker edge ice relative to the thinner ice in the transition zone. We found that the ice in the edge zone moved faster downwind than the interior ice, possibly due to its increased aerodynamic roughness. Once this ice moved away from the rest of the pack, the reflection and absorption of wind-wave energy, particularly at short periods, became even greater due to more developed seas at increased fetches. As shown below, the energy from both wind waves and swell contributes to the band formation. The bands then continue to move southwest until they melt under the action of warm water and waves.

b. The experiment

On the morning of 11 March, following a night of weak (4 m s^{-1}) easterly winds which compacted the ice edge, we used the helicopter to place six targets on ice floes. The targets were then tracked over a 23 h period with their positions determined from the Global Navigation System (GNS-500A) on the helicopter. Each target consisted of a colored nylon rectangle measuring approximately 1 m × 2 m which was nailed to the ice. Also, on three of the floes, we set up 2 m high wooden poles with radar reflectors mounted on top. Although we found that the reflector signal could not be distinguished from the ice on the radar of the ship, the poles served as good visual targets.

All of the floes tagged were initially within 3 km of the ice edge. Five of the floes tagged were snow-covered, rafted cakes measuring about 20 m × 15 m. Fig. 13 shows the appearance of one of these floes (green) shortly after the target was placed. The floe had a small ridge running down the middle with a rafted, snow-free area to the left. The sixth floe (blue) was a pancake measuring only 3 m × 5 m with slightly raised edges. Although we did not measure the bottom topography of these floes, the 0.4 m deep holes drilled for the poles did not reach bottom. We assume from our preceding discussion that the floe thicknesses were of order 1–5 m.

We initially placed the targets in a cross as shown at the top of Fig. 14. We then overflew the targets at 4, 9, and 23 h from the time of placement and recorded their positions. As Fig. 14 shows, not all of the floes were found at each overflight. For the same period, Table 1 shows the averaged wind data. The evolution of the targeted floes was as follows: When the targets were first placed, the ice edge was compact, with only a few ice cakes in the open water to the south. This was probably due to the weak easterly winds on the day preceding the experiment and to swell energy being reflected and absorbed by the ice. Fig. 15 is a photograph looking from the ice toward the open water at this time,

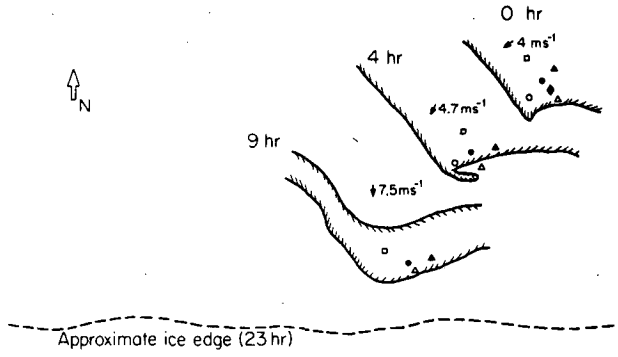

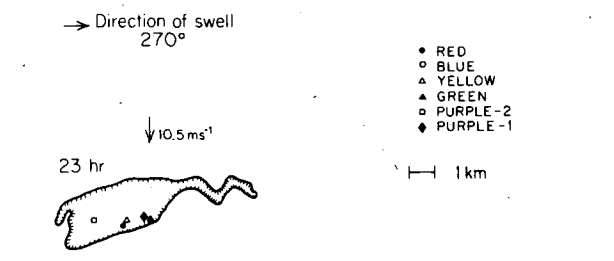

FIG. 14. A schematic diagram of the observed advance and relative positions of the targeted ice floes during the 23 h observation period. Floes are represented as shown in the ledger.

FIG. 15. Aerial view from 75 m looking toward the ice edge as it appeared just after the placement of the targets. The "blue" floe is barely visible in the middle of the photograph.

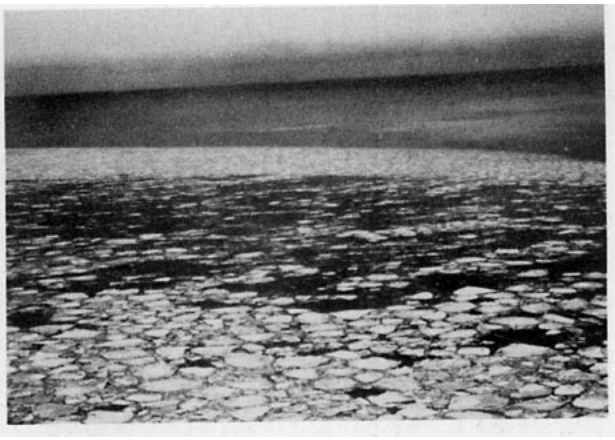

FIG. 16. Aerial view from 150 m of the ice edge as it appeared 4 h after the placement of the targets. The targeted ice floes were mostly located in the higher concentration of floes shown in the foreground.

where at least in the original photograph, the radar target mounted on the blue floe is visible in the middle of the picture.

At 4 h, after the wind began to pick up from the north, the targeted floes began to move away from the edge, creating as Fig. 16 shows, a band of 90% ice concentration outside of both an area of 25% concentration and a large, inner area of 90% concentration. As Fig. 14 shows, the outer ice band formed a hook outward from the pack ice. One floe (yellow) was in the 25% ice concentration region, while the other targets were in the inner high-concentration region.

At 9 h, which occurred at twilight so that photographs were impossible, all of the targeted floes were inside of a band of ice floes measuring 1–2 km across, which was located several hundred meters southwest of the main pack. This suggests the velocity of the floes in the band averaged 1×10^{-2} m s^{-1} faster than those in the pack. On our final survey at 23 h, which was in the morning of the next day, we observed many bands of ice similar to those shown in Fig. 12. As Fig. 14 shows, the targeted band was now ~15 km south of the ice edge, requiring the floes in the band to have moved overnight at an average velocity of 0.25 m s^{-1} faster than the pack. The band measured ~2 km wide at its widest part and 8–10 km in length. The band was widest at the end toward the swell and had a long, curving tail, which is shown in Fig. 17.

Fig. 18 shows the appearance of the head sighting against the direction of swell propagation. As with most bands observed, the downwind edges of the band were sharp. Because of the action of the swell and wind waves, the head and upwind edges were diffuse, consisting of a mixture of many small fragments of ice and larger, mostly submerged floes which were covered with small pieces of ice. To summarize, during our observational period the floes moved from 58°56.6′N, 170°4.7′W to 58°41.9′N, 170°22.4′W, so that they traveled 32 km in the direction 210°, or at ~25° to the right of the average wind, at an average speed of 0.38 m s^{-1}, or from Table 1 at 4% of the mean wind speed.

Although we cannot describe quantitatively the band formation and movement, we can carry out a scale analysis of the forces acting on the band

TABLE 1. Averaged wind data for the 23 h period.

Time period	Average speed (m s^{-1})	Average bearing (°T)
0–4	4.9	021
4–9	7.5	000
9–23	10.5	006
0–23	8.8	008

FIG. 17. An aerial view from 75 m of the tail of the band in Fig. 14, as it appeared 23 h after the target placement.

FIG. 18. A view from 25 m of the small fragments, pancakes and submerged floes at an edge of the band being acted on by wind and swell.

which drive it to the south. The problem divides into two parts: the initial movement of the band away from the pack ice, and its subsequent continued motion.

From our observations, the initial motion appears to be an effect of the increase in roughness of the floes near the edge, which leads to a greater aerodynamic drag. Because of our uncertainty about the relative water and air drag coefficients, we cannot show this quantitatively. Once the ice floes move away from the pack, however, their large velocity relative to the pack is very much an effect of the absorption and reflection of wind-generated waves.

To estimate the magnitudes of the forces on an ice floe away from the pack, we assume that the major forces acting on an ice floe are the aerodynamic wind drag, the hydrodynamic water drag, and the force created by the absorption and reflection of wind waves and swell. Using a quadratic stress law for the drag, the first two forces become

$$F_a = \rho_a C_a A \left|U_a - U_i\right|(U_a - U_i),$$

$$F_w = -\rho_w C_w A \left|U_i - U_w\right|(U_i - U_w),$$

where ρ is the density, C the drag coefficient, A the surface area of the floe, U the velocity, and the subscripts a, w, and i represent air, water and ice respectively. Banke *et al.* (1976) found the air-ice coefficient C_a to be $\sim 2 \times 10^{-3}$ for arctic ice and as large as 4.5×10^{-3} for sharp-edged pancakes. Therefore, for $U_a = 10$ m s^{-1}, $U_i = 0.4$ m s^{-1}, C_a of order 10^{-3}, and a typical floe of 400 m^2 surface area, F_a is of order 10^2 N, and is nearly independent of U_i.

In contrast, the water drag strongly depends on the quantity $(U_i - U_w)$. First, McPhee and Smith (1975) found a C_w of $\sim 3.4 \times 10^{-3}$ for fairly smooth, arctic ice. If we assume our rough ice (Fig. 6b) can be modeled as a bluff body (Schlichting, 1968, p. 623), then C_w is of order 10^{-2}. For this C_w and the same floe with $(U_i - U_w) = 0.1$ m s^{-1}, F_w is of order 10 N; while for $(U_i - U_w) = 0.4$ m s^{-1}, which corresponds to the observed case if U_w were zero, then F_w is of the order of 10^3 N. Therefore, the wind stress appears to be insufficient to move the ice at the observed velocity.

To estimate next the magnitude of the wave forcing, Longuet-Higgins (1977) shows that the force per unit width exerted on a floating body by waves is equal to $\frac{1}{4}\rho_w g(a^2 + a'^2 - b^2)$ where g is the gravitational acceleration, a the incident wave amplitude, and a' and b the reflected and transmitted amplitudes respectively. Wadhams (1973) from experiments with petri dishes in a wave tank, shows that the energy of short-period waves is almost all reflected or absorbed while that of longer period waves is mostly transmitted with an exponential energy decay with distance into the ice. Dean and Harleman (1966) also suggest that for stationary and moored obstacles, the reflection coefficients are generally quite large when the length of the obstacle is larger than half the incident wavelength. Using this criterion for a 20 m long ice floe in deep water, waves with periods ≤ 5 s will have large reflection coefficients. Therefore, estimates of the force exerted on a 20 m wide floe by totally reflected wind waves of various amplitudes are of order 10 N for $a = 0.01$ m, 10^3 N for $a = 0.1$ m, and 10^4 N for an amplitude of 0.3 m. For all but the smallest wave amplitudes, this forcing is greater or equal to the wind forcing. Depending on floe size then, wave forcing will increase as the fetch increases. Further, it will also increase if the ice floes in a band behave as a large floe and reflect the longer waves. The conclusion of this scale analysis is that once the floes move away from the pack, wave forcing causes them to move at a faster velocity than the pack interior.

Wave effects may also contribute to the relative motion of the ice in the band. As Fig. 14 shows, the floes were initially placed in a cross. During the first 4 h, motion of the floes was to the south or southwest relative to the purple-2 floe, represented by the square in Fig. 14. During the remaining 19 h, the relative motion was to the northeast. This latter change in relative position required a 2×10^{-2} m s^{-1} speed difference between the purple-2 floe and the others. The causes of this motion are unclear. The motion may have been largely diffusive; it may have been due in part to a shear zone occurring along the northeast–southwest axis of the band. The floes on the windward edge of the band are subject to wave forcing toward the southwest, which is greatest along the windward edge and decreases with distance into the band. Thus, windward floes are

forced slightly faster than leeward floes, resulting in relative motion along a northeast-southwest line.

c. *Consequences of the band motion*

Table 2, which lists the air temperature and water temperature, salinity and freezing point measured near the band, shows that as the ice band moved south, it moved into warmer, more saline water. At the beginning of our observations, the water temperature was −1.20°C, and the salinity was 31.9‰. At the end of the 23 h, the ice was in water of −0.45°C and a salinity of 32.2‰. In both cases, the freezing temperature of the water was ~−1.7°C. During this time, the air temperature decreased below the freezing point of the ice; a result of the northerly, off-ice winds of the Siberian high pressure system. However, because the water temperature ranged from +0.5 to +1.3°C above freezing, we observed the ice to melt.

Since the band was relatively long and narrow, lateral melting may have been of some importance, but vertical melting was most likely dominant due to the larger exposed surface area. By fracturing the floes, the waves create for each floe a larger ratio of surface area to volume which also yields increased melting. Also, waves breaking over the ice cause melting of the upper surface. As Fig. 18 shows, both fracturing and melting is visible along the windward and swellward edges of the band. Thus, the transport of ice in the form of long, thin bands of small floes into warmer water appears to be an efficient way to melt the pack ice.

Satellite images show the importance of this melting regime on a larger scale. Both Muench and Ahlnas (1976) and McNutt (1981) report, from viewing consecutive images, that floes in the pack ice interior move to the southwest throughout most of the eastern Bering Sea in late winter-early spring. The southern edge, however, does not appear to advance south during much of this time. This suggests that during periods of northeast winds the bands carry away enough ice to melt in the southwest to control the ice edge position.

TABLE 2. Water and air properties observed from the ship near the band.

Elapsed time (h)	Air temperature (°C)	Water temperature (°C)	Salinity (‰)	Freezing point (°C)
0	−0.70	−1.20	31.94	−1.73
4	−1.09	−1.30	32.05	−1.73
9	−1.79	−0.62	32.11	−1.73
23	−4.50	−0.45	32.23	−1.74
Average	−3.14	−0.60	32.11	−1.73

4. Conclusions

From analysis of satellite data, several investigators such as Campbell *et al.* (1975), Muench and Ahlnas (1976) and McNutt (1981) conclude that much of the ice in the Bering Sea forms in the north, then is conveyed to the southwest by the strong northeast winds which accompany the anticyclonic circulation of the Siberian high-pressure system. The present investigation of the southern ice edge processes shows in part how the ice edge position is maintained.

Basically, the large floes of the pack ice are advected southwest by the wind. As they approach the ice edge, the ocean swell propagating into the pack first fractures them into the characteristic rectangular pattern, then in the edge zone the floes are heavily rafted and ridged, which leads to a great increase in aerodynamic roughness. Because of this roughness increase, the ice in the edge zone moves away from the pack with greater relative velocity, and distributes itself into the characteristic bands. Enhanced by the absorption and reflection of wave momentum, these bands continue to move southwest into warmer water until they disintegrate. Further, the southward movement and disintegration of the bands exposes the transition zone to higher swell amplitudes, so that this zone becomes the edge zone and in turn becomes heavily rafted and ridged, so that it too blows southwest. In our case, a band moved 32 km in 23 h at an average speed of 0.38 m s^{-1} into water that was 1.3°C warmer than its freezing temperature. Thus the formation and movement of the ice bands are one method for the rapid dispersal and melting of the pack ice.

Acknowledgments. We thank Captain James G. Grunwell and the officers and crew of the NOAA ship *Surveyor* for their help in carrying out the field operations. We are particularly grateful to Lieutenant Bud Christman, the pilot of the Bell 206, who flew his helicopter in support of scientific operations for 10 of the 13 days which we spent at the ice front, and we thank the divers from the *Surveyor*, LCDR Turnbull, LT Williscroft, LTjg Fox and Mr. Kramer. Also, Mr. Peter Kauffman designed and built much of the equipment used in the field operations, and participated in most of the field work described in this paper. We greatly appreciate his support. We also thank Mr. William Abbott and Dr. Per Gloersen of the NASA Goddard Spaceflight Center for use of the photograph in Fig. 12. We finally thank Robert Lewis Charnell for his help during the planning phase of this ice edge experiment, and we deeply regret his loss at sea in December 1978. Most of this work was supported by the Bureau of Land Management through an interagency agreement with the National Oceanic and Atmospheric Administration, under which a multiyear

program responding to the needs of petroleum development of the Alaska continental shelf is managed by the Outer Continental Shelf Environmental Assessment Program (OCSEAP) office. S. Martin also gratefully acknowledges the support of the U.S. Department of Commerce Contract 78-4335 for the analysis of the ice core data, and J. Bauer also gratefully acknowledges the support of the Office of Naval Research Under Task No. NR307-252 and Contract N00014-76-C-0234. This is publication No. 1184 of the Department of Oceanography, University of Washington, and publication No. 558 of the Department of Atmospheric Sciences, University of Washington.

REFERENCES

Anonymous, 1973: U.S.-U.S.S.R. Bering Sea Expedition, Convair-990 Navigational Flight Data [Available from the Laboratory of Meteorology and Earth Sciences, Goddard Space Flight Center, Greenbelt, MD 20771].

Banke, E. G., S. D. Smith and R. J. Anderson, 1976: Recent measurements of wind stress on Arctic sea ice. *J. Fish. Res. Bd. Can.*, **33**, 2307–2317.

Campbell, W. J., P. Gloersen and R. O. Ramseier, 1975. Synoptic ice dynamics and atmospheric circulation during the Bering Sea experiment in *USSR/US Bering Sea Experiment*, K. Ya Kondratyev Ed., Gidrometeorizdat, 164–185.

——, R. O. Ramseier, R. J. Weaver and W. F. Weeks, 1977: Skylab floating ice experiment, Misc. Spec. Publi. No. 34, Department of Fisheries and the Environment, Fisheries and Marine Service, Ottawa 1977 [Available from Printing and Publishing Supplies and Services Canada, Ottawa, Canada, K1A 0S9].

Dean, R. G., and D. R. F. Harleman, 1966: Interactions of structures and waves. *Estuary and Coastline Hydrodynamics*, A. T. Ippen, Ed., McGraw-Hill, 341–403.

Gloersen, P., and P. E. LaViolette, 1974: Satellite imagery and weather for the BESEX area, 15 February through 10 March 1973. [Available through Technical Information Division, Code 250, Goddard Space Flight Center, Greenbelt, MD 20771].

Longuet-Higgins, M. S., 1977: The mean forces exerted by waves on floating or submerged bodies with applications to sand bars and wave power machines. *Proc. Roy. Soc. London*, **A352**, 463–480.

Martin, S., and P. Kauffman, 1979: Data report on the ice cores taken during the March 1979 Bering Sea ice edge field cruise on the NOAA ship *Surveyor*. [Available from OCSEAP, NOAA Project Office, P.O. Box 1808, Juneau, AK 99802].

McNutt, S. L., 1981: Remote sensing analysis of the ice regime in the eastern Bering Sea, March 1979. *Mon. Wea. Rev.*, **109** (in press).

McPhee, M. G., and J. D. Smith, 1975: Measurements of the turbulent boundary under pack ice. *AIDJEX Bull.*, No. 29, 49–92.

Muench, R. D., and K. Ahlnas, 1976: Ice movement and distribution in the Bering Sea from March to June 1974. *J. Geophys. Res.*, **81**, 4467–4476.

——, and R. L. Charnell, 1977: Observations of medium-scale features along the seasonal ice edge in the Bering Sea. *J. Phys. Oceanogr.*, **7**, 602–606.

Schlichting, H., 1968: *Boundary Layer Theory*. McGraw-Hill, 748 pp. (see p. 623).

Squire, V. A., and S. C. Moore, 1980: Direct measurement of the attenuation of ocean waves by pack ice. *Nature*, **283**, 365–368.

Wadhams, P., 1973: The effect of a sea ice cover on ocean surface waves. Ph.D. thesis, University of Cambridge, 223 pp.